Oscillation in Excited State Lifetimes with Size of Sub-Nanometer Neutral $(TiO_2)_n$ Clusters Observed with Ultrafast Pump-Probe Spectroscopy

Jacob M. Garcia,[1,2] Lauren F. Heald,[1,2] Ryan E. Shaffer,[1,2] and Scott G. Sayres[1,2,*]

1 School of Molecular Sciences, Arizona State University, Tempe, AZ 85287

2 Biodesign Center for Applied Structural Discovery, Arizona State University, Tempe, AZ 85287

KEYWORDS: Ultrafast dynamics, titanium oxide clusters, pump probe spectroscopy

Neutral titanium oxide clusters of up to 1 nm in diameter $(TiO_2)_n$, with $n < 10$, are produced in a laser vaporization source and subsequently ionized by a sequence of femtosecond laser pulses. Using 400 nm pump, 800 nm probe lasers, the excited state lifetimes of neutral $(TiO_2)_n$ clusters are measured. All clusters exhibit a rapid relaxation lifetime of ~30 fs, followed by a sub-picosecond lifetime that we attribute to carrier recombination. The excited state lifetimes oscillate with size, with even numbered clusters possessing longer lifetimes. Density functional theory calculations show the excited state lifetimes are correlated with electron-hole pair localization or polaron-like formation in the excited states of neutral clusters. Thus, structural rigidity is suggested as a feature for extending excited state lifetimes in titania materials.

Titania (TiO_2) is widely used due to its abundance, stability, low-cost and nontoxicity. It is also biologically compatible and chemically inert. These properties make it favorable for applications such as water splitting,[1,2] dye-sensitized solar cells,[3,4] white pigments,[5] environmental degradation of organic pollutants,[6] and heterogeneous photocatalysis.[7] TiO_2 is the archetypal photocatalytic material and serves as a model system for fundamental studies on the relationship between nuclear dynamics and the generation, transport, and trapping of charge carriers (electrons and holes) following photoexcitation. Absorption of a photon with energy exceeding the optical gap results in exciton formation, or bound electron-hole pair. Excitons can radiatively recombine or return to the ground state via nonradiative routes such as internal conversion, where excess energy dissipates as phonons or vibrations. The formation of photogenerated electrons and holes in titania is accompanied by lattice vibrations (phonons) that are quasiparticles collectively known as polarons. Small polaron formation occurs spontaneously in perfect lattices and acts to trap mobile carriers at recombination centers, decreasing their mobility[8] and affecting photoconversion yields.[9] Polaron formation ultimately impacts excited state dynamics, yet its detailed influence over lifetimes is not resolved.

Among the most important aspects of catalytic efficiency is the production of a photoexcited state with sufficient lifetime to enable chemical transformation. Ultrafast recombination of electrons and holes is the major efficiency loss mechanism and depends on strong electronic and electron-lattice correlations. Despite identical chemical compositions, the common polymorphs of bulk TiO_2 (rutile, anatase and brookite) exhibit different photocatalytic activities,[10–14] highlighting the critical role of local structure on the flow of energy. Polaron formation is favorable in the rutile phase, with carrier recombination two orders of magnitude faster than the anatase phase, where polaron formation is unfavorable and electrons remain delocalized.[12,14] Polarons formation in nanomaterials can accelerate electron/hole recombination through exciton self-trapping. Quantum confinement effects have not been observed in titania nanoparticles[15] as the sub-nanometer exciton binding radius[16,17] is smaller than the particle. The small exciton binding radius in titania makes sub-nanometer clusters the ideal venue for identifying the structural factors that govern carrier dynamics, electron-hole recombination mechanisms and related excited state lifetimes. Despite extensive research on TiO_2 nanoparticles, the excited state lifetimes at the ultimate size limit (clusters) have not yet been measured. Here, we utilize fs pump-probe spectroscopy to measure the excited state lifetimes of sub-nanometer titania clusters and apply computational studies to relate the dynamics to electron-hole separation and recombination.

Experimental lifetimes were measured using a home-built Wiley-McLaren[18] type time-of-flight mass spectrometer (TOF-MS) that was previously described.[19] A sub-35 fs Ti:Sapphire laser pulse was synchronized to the cluster beam to ionize the neutral clusters for detection. Mass spectra were recorded using 400 nm pump and 800 nm probe pulses with intensities of 9.9 x 10^{14} and 3.1 x 10^{15} W/cm^2, respectively. At temporal overlap, the largest ion signals were recorded from the neutral cluster distribution (Figure 1), consisting of both stoichiometric $(TiO_2)_n$ and suboxide clusters. Transient signals were fit using two exponential decay functions convoluted with a Gaussian function described elsewhere.[19,20] All clusters contain a fast (~35 fs) and a sub-picosecond relaxation component (Figure 2). The fast lifetime is attributed to an increase in signal that occurs through non-resonant excitation/ionization. As the laser pulses separate in time, the remaining ion signal is proportional to the neutral cluster's intermediate excited state population. The sub-picosecond excited state lifetime (τ) is attributed to rapid internal conversion returning to the S_0 state. The signal returns to baseline for all clusters, suggesting that carrier recombination is efficient for these sub-nm materials. The measured excited state

lifetimes oscillate with addition of TiO_2 units for cluster sizes from n = 1-7, with larger lifetimes observed for even-numbered clusters. Lifetimes gradually increase with size from 256 fs for n = 1 to ~550 fs for n > 6. Differences in excited state lifetimes are attributed to small changes in the local environment of each cluster that affect polaron formation.

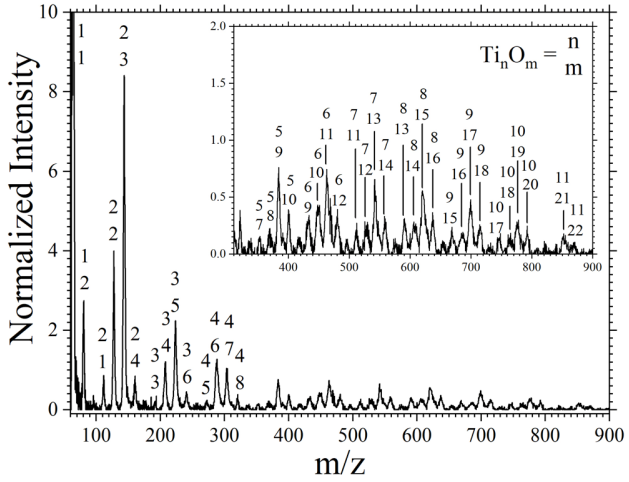

Figure 1. The mass spectrum of ionized neutral Ti_nO_m clusters at the temporal overlap of the 400 nm (pump) and 800 nm (probe) laser pulses.

Neutral $(TiO_2)_n$ cluster geometries were optimized at the DFT level within the Gaussian16 software suite[21] using the CAM-B3LYP[22] potential and standard 6-311G++ (3d2f, 3p2d) basis set. All clusters contain two terminal O atoms bound to a tetrahedral Ti atom, in agreement with literature assignments for the global minimum structures of $(TiO_2)_n$.[2,23–30] The stable conformations of clusters n > 4 possess all tetra-coordinated Ti atoms. Odd numbered clusters adopt C_s symmetry and even clusters adopt C_{2v} or C_{2h} symmetry. Stoichiometric $(TiO_2)_n$ are characterized as closed shell systems, where each O atom withdrawals two d-electrons from the Ti atoms, leaving the cluster void of d-electrons. Photoexcitation moves an electron from the occupied O 2p orbitals back to the unoccupied Ti 3d orbitals, analogous to the band structure of bulk TiO_2. The cluster's ionization potentials (IPs) and optical gaps have not been experimentally measured but are calculated to be ~10.0 ± 0.5 eV[24] and ~4.5 eV,[23] respectively (SI Table S1). Our results are consistent with photoexcitation by two pump photons (6.3 eV). The probe beam is maintained at threshold intensities to ensure the excess energy in the cations is less than a single probe photon (1.55 eV) and below the cation fragmentation energy.[24,31]

Excited state lifetimes are governed by electron-hole interactions, the magnitude of the transition energy, and nuclear motion. Time-dependent density functional theory (TD-DFT) calculations were performed to explore the excited states at the ground state (S_0) and adiabatically optimized excited state geometry (S_1). For simplicity, we limit our analysis to the S_1 state as a general description of photoexcitation. The S_1 state is the final state along the relaxation pathway and contains the biggest energy gap, suggesting it is the rate limiting step in relaxation. The large density of states and vibrational modes enables rapid internal conversion to the S_1 state in accordance with Kasha's rule.[32]

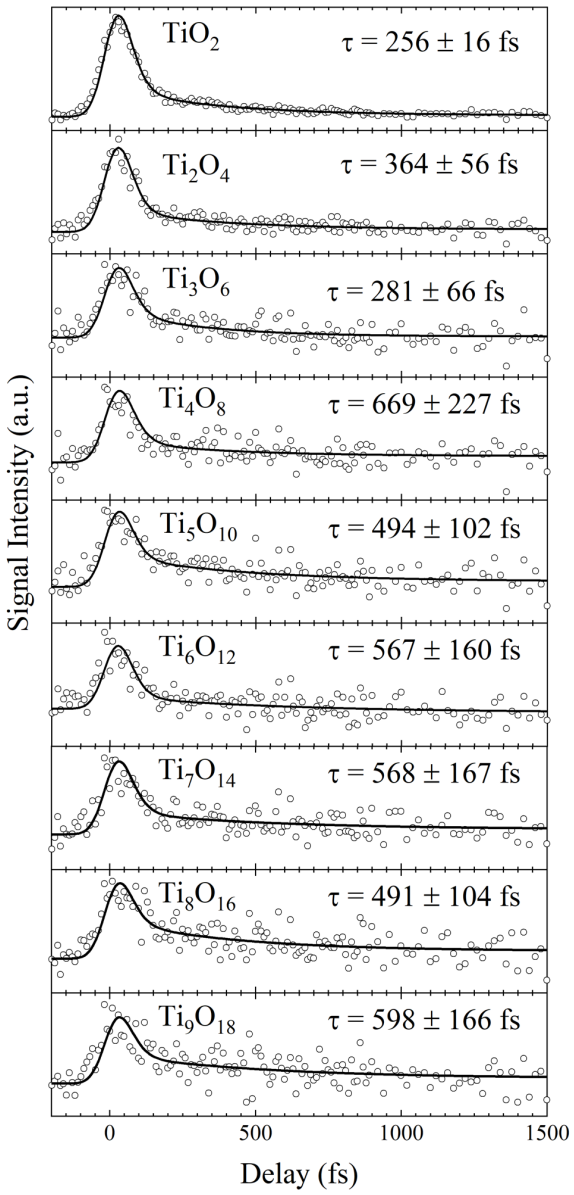

Figure 2. The transient spectra of the $(TiO_2)_n$ series as the intensity changes with probe delay. The total fit and long-lived lifetimes of each cluster is shown for n = 1 – 9.

To interpret the role of the electron-hole interactions on excited state lifetimes, several topological descriptors were calculated at both vertical excitation (S_0) and upon adiabatic relaxation to the S_1 minimum energy (SI Table S2). Photoexcitation involves several molecular orbitals, making transition densities (Figure 3) an efficient representation of the location and distribution of holes and electrons. The Λ index quantifies the charge-transfer character of excited states as the spatial overlap of electron and hole wavefunctions,[33–35] and ranges between 0 and 1 to describe wavefunctions that share no common space or complete overlap, respectively. Low Λ values suggest that the

exciton obtains a strong charge transfer character upon excitation and further increases on the S_1 landscape. The distance between electron and hole density centroids (d) is a complementary approach to measuring the charge-transfer length.[36] Although Λ and d are traditionally thought to relate to recombination lifetimes, neither parameter reconciles with the experimental lifetimes. Both values are small (Table 1), revealing that charges often localize on neighboring atoms without overlapping, thus demonstrating a large ionic character. These parameters are not reliable for such ionic systems and are poor predictors of excited state lifetimes for $(TiO_2)_n$ clusters.

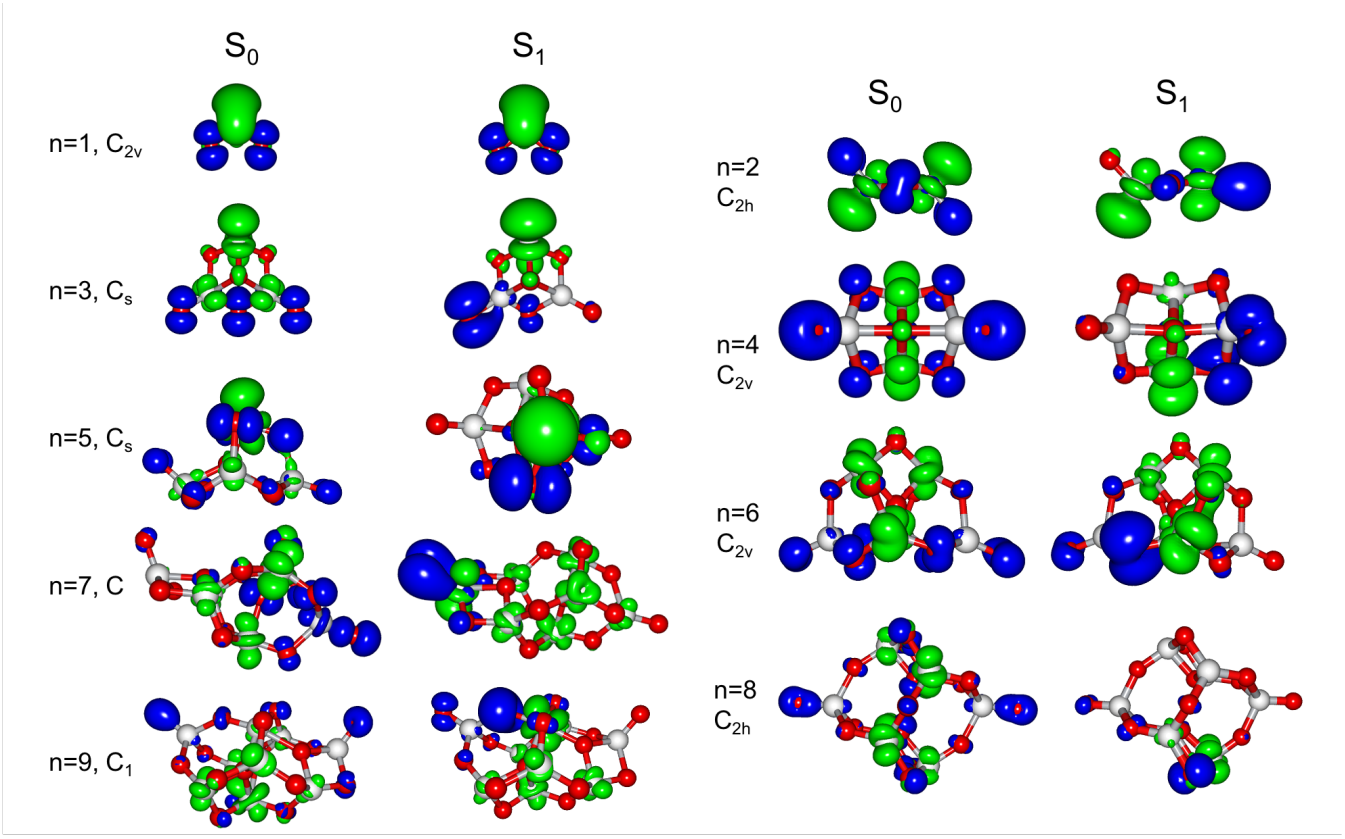

Figure 3. TD-CAM-B3LYP S_0 and S_1 transition densities for $(TiO_2)_n$, (n = 1-9), presented at an isodensity of 0.002 / Å^3. Electrons are shown in green, the hole is shown in blue, titanium atoms are white, and oxygen are red.

Upon photoexcitation, subtle changes in both the local geometry and electronic structure enable carrier localization and polaron formation which accounts for the measured lifetime oscillation. Theory shows the electronic structures of $(TiO_2)_n$ clusters exhibit an even/odd oscillation with additional TiO_2 units.[2,25,37] Even clusters have larger IPs, optical excitation energies (SI, Figure S1), and exciton binding energies (E_x) (SI, Figure S2). Larger energy spacings are indicative of more stable and rigid structures. The localization of each charge carrier is quantified by the total-root-mean-square density (σ_e and σ_h). The charge carriers are all delocalized upon vertical excitation, but in all cases, they separate (increasing d) and localize (decreasing σ) on the S_1 potential (SI Table 2). The experimental lifetime measurements, calculated topological parameters, and E_X are presented in Table 1. During adiabatic relaxation, both charge carriers show preference to localize on the least coordinated atoms. The under-coordinated Ti atom, typically found in the center of the cluster adjacent to a highly coordinated O atom, serves as the localization center for the electron density. If the hole overcomes the exciton binding energy, it migrates to a terminal O atom.

Structural rearrangement accompanies charge localization as the clusters relax through a Jahn-Teller (J-T) type distortion on S_1, similar to polaron formation in bulk structures. Due to the tetrahedral coordination of the Ti atoms, this results in a Ti-O bond elongation (Δr_{Ti-O}), which is more pronounced in even numbered clusters (SI, Figure S3). Although polarons are a bulk concept, the language is appropriate even for molecular-scale clusters due to the local structure deformation and localization of charge carriers. The polaron couples to the vibrational motion of the cluster and enables rapid depopulation by a radiationless transition through a conical intersection on the femtosecond timescale. In particular, the dangling O atoms are known to facilitate internal conversion.[38]

Variation in clusters provides a range of geometric configuration that mimic the active sites of bulk surfaces and can be utilized to understand the coupling between polaron formation and related lifetime changes. The formation of localized charge carriers and Coulomb attraction between the electron and hole

drives relaxation. In general, the odd numbered clusters are more planar in nature and exhibit shorter lifetimes than the even clusters. The higher symmetry and rigidity of even numbered clusters presents a more delocalized energy landscape where the S_0 transition density is distributed across all atomic centers, except those directly bound to the terminal O. Upon relaxation, the even numbered clusters show larger σ values that inhibits nonradiative decay pathways leading to longer lifetimes (Figure 4).

Table 1. Experimental excited state lifetimes (τ) and calculated properties for $(TiO_2)_n$ clusters.[a]

$(TiO_2)_n$	τ (fs)	Λ	d (Å)	σ_{av} (Å^3)	E_X (eV)	E_R (eV)
1	256 ± 16	0.26	1.73	3.31	5.33	0.11
2	364 ± 56	0.22	2.89	3.54	5.49	0.89
3	281 ± 66	0.14	4.16	2.83	2.69	1.29
4	669 ± 227	0.25	2.45	3.20	3.87	0.99
5	494 ± 102	0.24	1.81	3.11	3.75	0.86
6	567 ± 160	0.30	2.40	3.95	4.30	1.00
7	568 ± 167	0.25	3.90	4.40	4.08	1.00
8	491 ± 104	0.30	1.82	4.28	4.59	0.84
9	598 ± 164	0.35	2.50	4.31	3.89	1.10

[a]The topological descriptors for describing the character of the excited state: charge transfer character (Λ), distance between electron and hole density (d), average root mean standard deviation of the electron and hole (σ_{av}), and E_X and E_R. All presented values are for the S_1 state. The relaxation energy (E_R) is the difference in energy between the optimized geometries at the S_0 and S_1 states.

The smallest three clusters are planar, feature under-coordinated Ti atoms, and exhibit the shortest lifetimes. TiO_2 and $(TiO_2)_2$ are too small to enable carrier separation and therefore have large E_X. Following excitation, $(TiO_2)_2$ adopts a more planar geometry as the hole localizes on a terminal O atom. $(TiO_2)_3$ is unique in that it contains a three-fold coordinated Ti and O. The electron density moves onto the 3d orbital of the under-coordinated Ti atom and the hole localizes on the opposite side of the cluster. $(TiO_2)_3$ has the smallest S_1 energy gap, and the largest E_R which are strong drivers for recombination.

An increase in lifetime occurs as the clusters move to a 3D structure and feature Ti atoms that are all tetracoordinated. Both $(TiO_2)_4$ and $(TiO_2)_5$ structures contain a tetra-coordinated O atom with ionic character which provides rigidity.[24] Upon adiabatic relaxation, the electron of $(TiO_2)_4$ localizes on one Ti, but the hole behaves as a multi-site polaron distributed about two O atoms causing a large local bond elongation (0.30 Å). On the S_0 landscape of $(TiO_2)_5$, the electron resides on the Ti furthest from the terminal O, the hole arises from the three adjacent O atoms, while the majority of the cluster is inactive. Upon adiabatic relaxation on S_1, the hole localizes to one O forming an exciton pair that reduces the excited state lifetime.

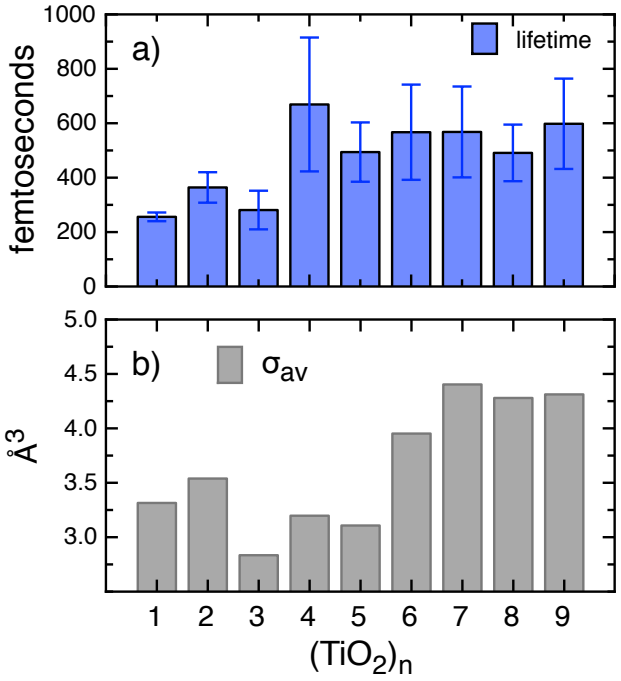

Figure 4. Comparative plots showing the a) experimental lifetime and b) TD-DFT averaged electron and hole distributions of $(TiO_2)_n$ clusters on the excited state.

As the cluster size increases above $(TiO_2)_6$, the oscillation is less apparent, and lifetimes approach a similar value. $(TiO_2)_6$ exhibits a low number of vibrational bands,[30] highlighting a rigid structure that contains a tetra-coordinated O in its center. Similar to $(TiO_2)_4$, $(TiO_2)_6$ does not exhibit electron localization, thus prolonging its lifetime. Despite having a collection of hole and electron on adjacent atoms following relaxation, the distortion in both clusters occurs primarily through elongation of one Ti-O bond, while the remaining cluster is rigid.

Both $(TiO_2)_5$ and $(TiO_2)_8$ exhibit relatively low E_R, resulting in a strong localization of both carriers into a bound exciton (Ti^{3+}-O^-) pair, which facilitates internal conversion. The centrosymmetric S_0 state of $(TiO_2)_8$ contains delocalized charge carriers spread over the entire cluster. $(TiO_2)_8$ has the largest E_{ex}, where the S_1 structure migrates the electron and hole to adjacent atoms in the middle of the cluster (d = 1.82 Å) and contains a large Λ (0.30), supporting a shortened lifetime (491 fs). Both of these clusters have a ‘‘glassy’’ energy landscape and exhibit a large number of low-energy isomers.[26] Their flexible structures enable charge localization and rapid relaxation.

In $(TiO_2)_7$ and $(TiO_2)_9$, the hole migrates to a trapped site, leaving a delocalized electron in the core of the cluster due to a small E_{ex}. In $(TiO_2)_7$, both charge carriers are delocalized, but on opposite ends of the cluster. The S_1 relaxation mechanism is similar to $(TiO_2)_2$, where the hole localizes on the terminal O and becomes more planar. The remaining cluster is unperturbed, inhibiting electron polaron formation (σ_e= 5.86 Å). This separation reduces slows recombination to break the oscillating trend, and instead exhibits a similar lifetime to $(TiO_2)_6$. The breakdown in oscillation occurs at similar size regime as the

onset of bulk-like energy gaps.[17] $(TiO_2)_9$ contains a highly coordinated center (six-fold coordinated Ti and several tri-coordinated O atoms) that attracts both charge carriers on S_1. Although the hole forms a multicenter polaron, the electron does not localize (σ_e = 4.94 Å), and therefore exhibits a similar lifetime to the other delocalized clusters.

This experiment identifies key molecular-level parameters that can be applied to aid new synthetic strategies to design materials, surfaces, and coatings with extended excited state lifetimes and improved photocatalytic performance. The tightly bound carriers (d < 0.5 nm) are in agreement with simulations of larger nanoparticles.[39] Thus, slightly increasing the cluster size into the few nanometer size regime will likely not impact the excited state lifetimes significantly, as the carriers do not utilize all the space in clusters this small. These clusters capture the important features and therefore are adequate mimics of bulk systems. The electron localizes on the lowest coordinated Ti, analogous to the electron trapping on under-coordinated Ti^{3+} cation centers that accompany O defect sites on bulk surfaces. Additionally, the electron typically does not localize on a single site unless bound to a hole in an exciton pair. These results suggest that prolonged excited states lifetimes (and related excitons) can be achieved by preparing bulk surfaces that more closely mimic the structural features of the clusters.

The excited state lifetimes of neutral $(TiO_2)_n$ clusters were measured using femtosecond pump-probe spectroscopy to be sub-picosecond in duration. We show the cluster's excited-state lifetimes reach a steady value as they approach the ~1 nm size regime, with similar values (τ~550 fs) recorded for clusters of n ≥ 7. The tightly bound electron-hole pairs are consistent with the sub-nanometer exciton binding radius found in bulk structures. The oscillation in lifetimes as clusters grow in size is attributed to structural differences between the clusters that control charge localization and polaron formation. Time-dependent density functional calculations show the increased lifetime for even clusters is associated with a more rigid structure, lower electron-hole pair localization, and extended bond lengths. We show that polaron formation shortens excited state lifetimes. Therefore, the utilization of rigid structures which inhibits polaron formation is essential for the production of titanium oxide materials containing longer excited state lifetimes.

SUPPORTING INFORMATION

Computational methods and properties calculated at both the ground and excited state. Table S1 shows the ionization potentials, electron affinities, optical gaps. Table S2 shows the topological descriptors (Λ, d, σ). Table S3 contains the exciton binding energies, relaxation energies, and changes in bond length. The material is free of charge via the Internet at http://pubs.acs.org.

Corresponding Author

*Scott.Sayres@asu.edu

Author Contributions

S.G.S and JMG designed the experiments. JMG and RES performed the ultrafast pump-probe spectroscopy, SGS and LFH performed the theoretical calculations, and SGS and JMG wrote the paper with contributions from all authors.

Acknowledgements

We gratefully acknowledge support from ASU Lightworks. J.G also acknowledges support from Western Alliance to Expand Student Opportunities (WAESO) Louis Stokes Alliance for Minority Participation (LSAMP) Bridge to Doctorate (BD) National Science Foundation (NSF) Grant No. HRD-1702083.

References

(1) Xu, H. G.; Li, X. N.; Kong, X. Y.; He, S. G.; Zheng, W. J. Interaction of TiO^+ with Water: Infrared Photodissociation Spectroscopy and Density Functional Calculations. *Phys. Chem. Chem. Phys.* **2013**, *15*, 17126–17133.

(2) Çakir, D.; Gülseren, O. Ab Initio Study of Neutral $(TiO_2)_n$ Clusters and Their Interactions with Water and Transition Metal Atoms. *J. Phys. Condens. Matter* **2012**, *24*, 305301.

(3) Oprea, C. I.; Gîrțu, M. A. Structure and Electronic Properties of TiO 2 Nanoclusters and Dye–Nanocluster Systems Appropriate to Model Hybrid Photovoltaic or Photocatalytic Applications. **2019**, *9*, 357.

(4) Chou, T. P.; Zhang, Q.; Russo, B.; Fryxell, G. E.; Cao, G. Titania Particle Size Effect on the Overall Performance of Dye-Sensitized Solar Cells. *J. Phys. Chem. C* **2007**, *111*, 6296–6302.

(5) Siwi Nska-Stefa Nska, K.; Nowacka, M.; Ko1odziejczak-Radzimska, A.; Jesionowski, T. Preparation of Hybrid Pigments via Adsorption of Selected Food Dyes onto Inorganic Oxides Based on Anatase Titanium Dioxide. *Dye. Pigment.* **2012**, *94*, 338–348.

(6) Muraca, A. R.; Kershis, M. D.; Camillone, N.; White, M. G. Ultrafast Dynamics of Acetone Photooxidation on TiO_2(110). *J. Chem. Phys.* **2019**, *151*, 161103.

(7) Rastogi, A.; Zivcak, M.; Sytar, O.; Kalaji, H. M.; He, X.; Mbarki, S.; Brestic, M. Impact of Metal and Metal Oxide Nanoparticles on Plant: A Critical Review. *Front. Chem.* **2017**, *5*, 78.

(8) Richter, C.; Schmuttenmaer, C. A. Exciton-like Trap States Limit Electron Mobility in TiO_2 Nanotubes. *Nat. Nanotechnol.* **2010**, *5*, 769–772.

(9) Shingai, D.; Ide, Y.; Sohn, W. Y.; Katayama, K. Photoexcited Charge Carrier Dynamics of Interconnected TiO_2 Nanoparticles: Evidence of Enhancement of Charge Separation at Anatase-Rutile Particle Interfaces. *Phys. Chem. Chem. Phys.* **2018**, *20*, 3484–3489.

(10) Luttrell, T.; Halpegamage, S.; Tao, J.; Kramer, A.; Sutter, E.; Batzill, M. Why Is Anatase a Better Photocatalyst than Rutile? - Model Studies on Epitaxial TiO_2 Films. *Sci. Rep.* **2015**, *4*, 1–8.

(11) Zhang, J.; Zhou, P.; Liu, J.; Yu, J. New Understanding of the Difference of Photocatalytic Activity among Anatase, Rutile and Brookite TiO_2. *Phys. Chem. Chem. Phys.* **2014**, *16*, 20382–20386.

(12) Maity, P.; Mohammed, O. F.; Katsiev, K.; Idriss, H. Study of the Bulk Charge Carrier Dynamics in Anatase and Rutile TiO_2 Single Crystals by Femtosecond Time-Resolved Spectroscopy. *J. Phys. Chem. C* **2018**, *122*, 8925–8932.

(13) Obara, Y.; Ito, H.; Ito, T.; Kurahashi, N.; Thürmer, S.; Tanaka, H.; Katayama, T.; Togashi, T.; Owada, S.; Yamamoto, Y. I.; et al. Femtosecond Time-Resolved X-Ray Absorption Spectroscopy of Anatase TiO_2 Nanoparticles Using XFEL. *Struct. Dyn.* **2017**, *4*.

(14) Elmaslmane, A. R.; Watkins, M. B.; McKenna, K. P. First-Principles Modeling of Polaron Formation in TiO_2 Polymorphs. *J. Chem. Theory Comput.* **2018**, *14*, 3740–3751.

(15) Monticone, S.; Tufeu, R. .; Kanaev, A. V. .; Scolan, E. .; Sanchez, C. . Quantum Size Effect in TiO_2 Nanoparticles: Does It Exist? *Appl. Surf. Sci.* **2000**, *162–163*, 565–570.

(16) Serpone, N.; Lawless, D.; Khairutdinov, R. Size Effects on the Photophysical Properties of Colloidal Anatase TiO_2 Particles: Size Quantization or Direct Transitions in This Indirect Semiconductor? *J. Phys. Chem.* **1995**, *99*, 16646–16654.

(17) Zhai, H. J.; Wang, L. S. Probing the Electronic Structure and Band Gap Evolution of Titanium Oxide Clusters $(TiO_2)_n^-$ (n = 1-10) Using Photoelectron Spectroscopy. *J. Am. Chem. Soc.* **2007**,

129, 3022–3026.

(18) W. C. Wiley and I. H. McLaren. Time-of-Flight Mass Spectrometer with Improved Resolution. *Rev. Sci. Instrum.* **1955**, *26*, 1150–1157.

(19) Garcia, J. M.; Shaffer, R. E.; Sayres, S. G. Ultrafast Pump-Probe Spectroscopy of Finite-Sized Neutral Iron Oxide Clusters. **2020**, *22*, 24624–24632.

(20) Dermota, T. E.; Hydutsky, D. P.; Bianco, N. J.; Castleman, A. W. Excited-State Dynamics of $(SO_2)_m$ Clusters. *J. Phys. Chem. A* **2005**, *109*, 8259–8267.

(21) Frisch, M. J.; Trucks, G. W.; Schlegel, H. B.; Scuseria, G. E.; Robb, M. A.; Cheeseman, J. R.; Scalmani, G.; Barone, V.; Mennucci, B.; Petersson, G. A.; et al. Gaussian16 (Revision A.03), Gaussian Inc. Wallingford CT. 2016.

(22) Yanai, T.; Tew, D. P.; Handy, N. C. A New Hybrid Exchange-Correlation Functional Using the Coulomb-Attenuating Method (CAM-B3LYP). *Chem. Phys. Lett.* **2004**, *393*, 51–57.

(23) Berardo, E.; Hu, H. S.; Shevlin, S. A.; Woodley, S. M.; Kowalski, K.; Zwijnenburg, M. A. Modeling Excited States in TiO_2 Nanoparticles: On the Accuracy of a TD-DFT Based Description. *J. Chem. Theory Comput.* **2014**, *10*, 1189–1199.

(24) Qu, Z. W.; Kroes, G. J. Theoretical Study of the Electronic Structure and Stability of Titanium Dioxide Clusters $(TiO_2)_n$ with n = 1-9. *J. Phys. Chem. B* **2006**, *110*, 8998–9007.

(25) Ganguly Neogi, S.; Chaudhury, P. Structural, Spectroscopic Aspects, and Electronic Properties of $(TiO_2)_n$ Clusters: A Study Based on the Use of Natural Algorithms in Association with Quantum Chemical Methods. *J. Comput. Chem.* **2014**, *35*, 51–61.

(26) Marom, N.; Kim, M.; Chelikowsky, J. R. Structure Selection Based on High Vertical Electron Affinity for TiO_2 Clusters. *Phys. Rev. Lett.* **2012**, *108*.

(27) Li, S.; Dixon, D. A. Molecular Structures and Energetics of the $(TiO_2)_n$ (n = 1-4) Clusters and Their Anions. *J. Phys. Chem. A* **2008**, *112*, 6646–6666.

(28) Lamiel-Garcia, O.; Cuko, A.; Calatayud, M.; Illas, F.; Bromley, S. T. Predicting Size-Dependent Emergence of Crystallinity in Nanomaterials: Titania Nanoclusters: Versus Nanocrystals. *Nanoscale* **2017**, *9*, 1049–1058.

(29) Calatayud, M.; Maldonado, L.; Minot, C. Reactivity of $(TiO_2)_N$ Clusters (N = 1-10): Probing Gas-Phase Acidity and Basicity Properties. *J. Phys. Chem. C* **2008**, *112*, 16087–16095.

(30) Weichman, M. L.; Song, X.; Fagiani, M. R.; Debnath, S.; Gewinner, S.; Schöllkopf, W.; Neumark, D. M.; Asmis, K. R. Gas Phase Vibrational Spectroscopy of Cold $(TiO_2)_n^-$ (n = 3-8) Clusters. *J. Chem. Phys.* **2016**, *144*, 124308.

(31) Jeong, K. S.; Chang, C.; Sedlmayr, E.; Sülzle, D. Electronic Structure Investigation of Neutral Titanium Oxide Molecules Ti_xO_Y. *J. Phys. B At. Mol. Opt. Phys.* **2000**, *33*, 3417–3430.

(32) Kasha, M. Characterization of Electronic Transitions in Complex Molecules. *Discuss. Faraday Soc.* **1950**, *9*, 14–19.

(33) Berardo, E.; Hu, H. S.; Van Dam, H. J. J.; Shevlin, S. A.; Woodley, S. M.; Kowalski, K.; Zwijnenburg, M. A. Describing Excited State Relaxation and Localization in TiO_2 Nanoparticles Using TD-DFT. *J. Chem. Theory Comput.* **2014**, *10*, 5538–5548.

(34) Peach, M. J. G.; Benfield, P.; Helgaker, T.; Tozer, D. J. Excitation Energies in Density Functional Theory: An Evaluation and a Diagnostic Test. *J. Chem. Phys.* **2008**, *128*, 044118.

(35) Valero, R.; Morales-Garciá, Á.; Illas, F. Investigating the Character of Excited States in TiO_2 Nanoparticles from Topological Descriptors: Implications for Photocatalysis. *Phys. Chem. Chem. Phys.* **2020**, *22*, 3017–3029.

(36) Mewes, S. A.; Plasser, F.; Krylov, A.; Dreuw, A. Benchmarking Excited-State Calculations Using Exciton Properties. *J. Chem. Theory Comput.* **2018**, *14*, 710–725.

(37) Rana, T. H.; Kumar, P.; Solanki, A. K.; Skomski, R.; Kashyap, A. Ab-Initio Study of Free Standing TiO_2 Clusters: Stability and Magnetism. *J. Appl. Phys.* **2013**, *113*.

(38) Peng, W. T.; Fales, B. S.; Shu, Y.; Levine, B. G. Dynamics of Recombination: Via Conical Intersection in a Semiconductor Nanocrystal. *Chem. Sci.* **2018**, *9*, 681–687.

(39) Fazio, G.; Ferrighi, L.; Di Valentin, C. Photoexcited Carriers Recombination and Trapping in Spherical vs Faceted TiO_2 Nanoparticles. *Nano Energy* **2016**, *27*, 673–689.

Insert Table of Contents artwork here